A chemical-mechanical ex-situ aging of perfluorosulfonic-acid membranes for fuel cells: impact on the structure and the functional properties

Mylène Robert, Assma El Kaddouri, Marie Crouillere, Jean-Christophe Perrin, Laetitia Dubau, Florence Dubelley, Kévin Mozet, Meriem Daoudi, Jérôme Dillet, Jean-Yves Morel, et al.

A chemical-mechanical *ex-situ* aging of perfluorosulfonic-acid membranes for fuel cells: impact on the structure and the functional properties

Mylène Robert[a,*], Assma El Kaddouri[a], Marie Crouillere[b], Jean-Christophe Perrin[a], Laetitia Dubau[b], Florence Dubelley[b], Kévin Mozet[a], Meriem Daoudi[a], Jérôme Dillet[a], Jean-Yves Morel[a], Sébastien Leclerc[a], Olivier Lottin[a]

[a] *Université de Lorraine, CNRS, LEMTA, F-54000 Nancy, France*

[b] *Univ. Grenoble Alpes, Univ. Savoie Mont Blanc, CNRS, Grenoble INP, LEPMI, 38000 Grenoble, France*

* *Corresponding author*

E-mail addresses: mylene.robert@univ-lorraine.fr (M. Robert), assma.el-kaddouri@univ-lorraine.fr (A. El Kaddouri), marie.crouillere@univ-smb.fr (M. Crouillere), jean-christophe.perrin@univ-lorraine.fr (J.-C. Perrin), laetitia.dubau@grenoble-inp.fr (L. Dubau), florence.dubelley@univ-smb.fr (F. Dubelley), kevin.mozet@univ-lorraine.fr (K. Mozet), meriem.daoudi@univ-lorraine.fr (M. Daoudi), jerome.dillet@univ-lorraine.fr (J. Dillet), jean-yves.morel@univ-lorraine.fr (J.Y. Morel), sebastien.leclerc@univ-lorraine.fr (S. Leclerc) , olivier.lottin@univ-lorraine.fr (O. Lottin).

Abstract

Perfluorosulfonic acid (PFSA) membranes are key components for the operation of Polymer Electrolyte Membrane Fuel Cells (PEMFC). They undergo harsh conditions in terms of chemical environment and mechanical fatigue leading to irreversible degradations, up to their failure and to the Fuel Cell (FC) shutdown in worst cases. Through an *ex-situ* approach, this study aims to provide new insights about the impact of conjoint mechanical and chemical stresses on the structure and the functional properties of PFSA membranes. In this regard, various aging tests have been carried out using a custom-made device able to combine the application of a mechanical stress (sinusoidal profile) and the exposure to an environment containing free radicals (*i.e.* Fenton's reagents). After about twenty hours of accelerated aging test the analysis of the aged membranes permitted to demonstrate that the exposure to the combined stress significantly altered the morphology of Nafion™ XL membrane, with the appearance of bubbles close to the membrane surface and even delamination at the PFSA/reinforcement interface. On the other hand, and rather paradoxically, the water sorption and self-diffusion properties of the aged membranes as well as their cell performances remained satisfactory.

Keywords:

Chemical degradation; Durability; Mechanical fatigue; Nafion™ membrane; Water mobility; Water sorption

1. Introduction

Perfluorosulfonic-acid (PFSA) membranes used in Proton Exchange Membrane Fuel Cells (PEMFC) still suffer from severe damages after long-term operation [1–4]. They are particularly sensitive to some specific operating conditions like low currents or Open Circuit Voltage (OCV) as well as rapid humidity cycling because of the mechanical fatigue it can engender: such stressors affects the membrane stability and leads to polymer chemical decomposition, membrane thinning, and/or formation and growth of creeps, cracks, or pinholes [5–7]. In addition, PFSA membranes are exposed to aggressive environments resulting from the formation of hydrogen peroxide and its decomposition into free radicals such as hydrogen ($H^{\bullet}$), hydroxyl ($HO^{\bullet}$) or hydroperoxyl ($HOO^{\bullet}$) radicals [4,8,9]. These species attack the weakest bonds of the polymer chains (backbone and/or side chains) and alter the structure and the mechanical integrity of the membrane, leading to its thinning and the appearance of defects [10–13]. The repeated swelling/shrinkage events imposed by the humidity cycling generates alternatively compressive and tensile stresses in the membrane [14–17] and the accumulation of these residual stresses can then generates the growth of cracks and pinholes [12,13,18,19]… which, in turns, increases gas crossover and the generation of radicals.

Despite innumerable studies focusing independently on chemical or mechanical degradations, only a few recent works were related to the effect of the coupled mechanical and chemical degradation on PFSA membranes [20–28]. Kusoglu *et al.* analyzed the effect of compressive stress on the chemical degradation of Nafion™ membrane through an *ex-situ* approach [21]. They demonstrated that polymer decomposition increases in a non-linear way with the compression level, suggesting a synergistic nature of chemical and mechanical stresses. Thanks to SAXS measurements, their work also showed that under compression, the chemical degradation led to a significant modification of PFSA microstructure with an increase of the spacing between water domains in the membrane. However, Kusoglu *et al.* exposed membranes to a static mechanical pressure, which represents only one aspect of the solicitations exerted in fuel cell.

Recently, specific *in-situ* accelerated stress tests (AST) were developed to study the impact of coupled mechanical and chemical stress on PFSA membranes and better replicate field operating conditions [23–28]. They consist in applying alternatively OCV phases – to induce chemical stress – and periodic wet/dry cycles – to induce mechanical stress – thus allowing to evaluate membrane durability with a significantly reduced time to failure [23]. *In-situ* cyclic open circuit voltage (COCV) AST significantly accelerate the overall membrane degradation: fluorine emissions and membrane thinning increase with the number of COCV cycles [23–25]. In addition, an important decay of the membranes' mechanical properties, *i.e.* fracture strain and elastic modulus, was observed as a result of combined mechanical/chemical AST: the polymer structure tends to become stiffer, more brittle, and thus more vulnerable to cracks/pinholes initiation [23,24,28]. Venkatesan *et al.* [25] observed localized membrane degradation induced by COCV at the mesoscale, believed to evolve into macroscopic damage. The authors identified localized regions depleted from fluorine, carbon and oxygen,

suggesting ionomer loss, as well as ion-cluster voids growing into microcracks. More recently, Ramani *et al.* [28] developed a novel non-destructive method for 3D analysis of membrane failure using X-ray computed tomography (XCT). They thus identified a new membrane failure mode due to COCV: the development of cracks through the membrane's thickness which were structurally independent from catalyst layers cracks. Furthermore, in order to understand the effect of conjoint chemical-mechanical degradations compared to conventional isolated stresses, Mukundan *et al.* [26] studied three types of *in-situ* AST in comparison with field testing: OCV AST, relative humidity cycling (RHC) AST and OCV RHC AST. OCV AST induced a significant change in ionomer crystallinity and membrane thinning, but no crack was observed. RHC AST replicated mechanical failure with observable PEM cracks but no further damage or gas crossover were detected. With OCV RHC testing, membrane failure was reached after only few hundred hours and led to PEM cracking, membrane thinning and gas crossover. Moreover, the degradations observed after OCV RHC were similar to those undergone by MEA during in-field operation, while, on the one hand, OCV AST overestimates the chemical degradation impact during the test and RHC AST may not be aggressive enough to provide accelerated degradation.

Finally, it must be kept in mind that the membranes functional properties are strongly related to their microstructure and morphology [29,30] so that the fundamental understanding of their aging mechanisms may also help to improve their performance as well as water management in FC [31–33]. Among the different aging mitigation strategies developed in recent years, the use of a microporous polytetrafluoroethylene (PTFE) reinforcement layer on the one hand, and the use of cerium-based radical scavengers on the other hand have improved the mechanical and chemical stability of membranes, while maintaining sufficient proton conductivity [34–36]. Nevertheless, such composite membranes still undergo significant degradations during operation [26,37,38].

In a previous work, we designed a specific device able to couple the exposure to an aggressive chemical environment (*i.e.* free radicals) with a cyclic compressive stress – in conditions representative of FC operation – through an *ex-situ* approach [39]. First results showed an acceleration of Nafion™ membranes degradation: an increase of the fluorine emission rate and of the hydrogen permeation current was observed, suggesting that some microstructural changes may appear through the membranes during the experiments. However, the aging tests consisted only in the application of a 5 MPa cyclic compressive stress coupled to the exposure to H_2O_2 or Fenton solutions. Additional aging tests were performed in the present work to further investigate the impact of coupled chemical-mechanical stress on membranes by varying the type of compressive stress (static or cyclic), the pressure level (0, 5 or 10 MPa), the chemical stress level (H_2O_2 or Fenton solution) and the aging duration (8 or 20 hours). Cyclic compression was applied to reproduce the swelling/shrinkage sequences imposed by the membrane water-uptake during transient FC operation while a static compressive stress was applied for comparison, and to reproduce the stack clamping pressure. Furthermore, deeper analyses were carried out to examine more specifically the effects of a conjoint mechanical and chemical stress on the morphology, the structure, and the functional

properties of Nafion™ membranes. Analyses by Scanning Electron Microscopy (SEM) and ^{19}F-NMR spectroscopy were performed to study the evolution of the morphology and chemical structure of aged membranes at the microscopic and the polymer repeat unit scales, respectively. The water sorption capacity and the self-diffusion coefficient were also measured in order to evaluate the impact of the chemical-mechanical aging on functional properties of membranes.

2. Experimental

2.1 Material and preparation

Nafion™ NR211 and Nafion™ XL were purchased from Ion Power Inc. Both are PFSA membranes elaborated from the copolymerization of perfluoro(4-methyl-3,6-dioxa-7-octene-1-sulfonyl fluoride) and tetrafluoroethylene (TFE) with similar Ion Exchange Capacity (IEC) – 0.98 ± 0.03 meq.g^{-1} for the NR211 and 0.92 ± 0.03 meq.g^{-1} for the XL – and nominal thicknesses – 25.4 µm for the NR211 *vs.* 27.5 µm for the XL –. The XL membrane differs from the NR211 by the presence of additional PTFE-rich reinforcement and cerium-based radical scavengers.

The membrane samples were pretreated using a procedure comparable to the one established by Xu *et al.* [40] In addition, after the acidification step proposed by the authors, the cleaned membrane samples were washed in deionized water at 80 °C for one hour to remove eventual excess of acid solution, then dried in an oven at 60 °C for 24 hours.

2.2 Experimental setup

The specific device (Fig. 1) and the operating conditions used for the mechanical-chemical aging tests performed in this study are identical to that described in our previous work [39].

To induce chemical degradation, a solution (H_2O_2 or Fenton solutions) circulates at a continuous flow rate of 3.0 mL.min^{-1} through the two half-cells, ensuring a residence time of about 10 seconds per half-cell. This value was chosen for three main reasons:

- to guarantee a sufficient pre-heating of the solution before it reaches the membrane.
- to be able to store enough solution in the upstream and downstream containers (5 L each) so that the degradation protocols could be performed during 8 hours without human intervention.
- to guarantee fast renewal of the solution in contact with the membrane: the solution was renewed every two cycles, *i.e.* every 20 seconds.

The mechanical stress was either static or cyclic compressive stress. In the case of cyclic solicitations, the frequency of 0.1 Hz was chosen to be significantly higher than the characteristic diffusion time of water through the membrane, estimated to be approximately 1.0-1.2 seconds assuming a water self-diffusion coefficient of about 6.10^{-10} m².s^{-1} in fully hydrated membranes. Such a cyclic mechanical stress can be considered as quite severe:

0.1 Hz during 8 to 20 hours is roughly equivalent to 8 to 20 years of daily operation, assuming a fuel cell startup and shutdown per day (*i.e.* 360 swelling/shrinkage cycles).

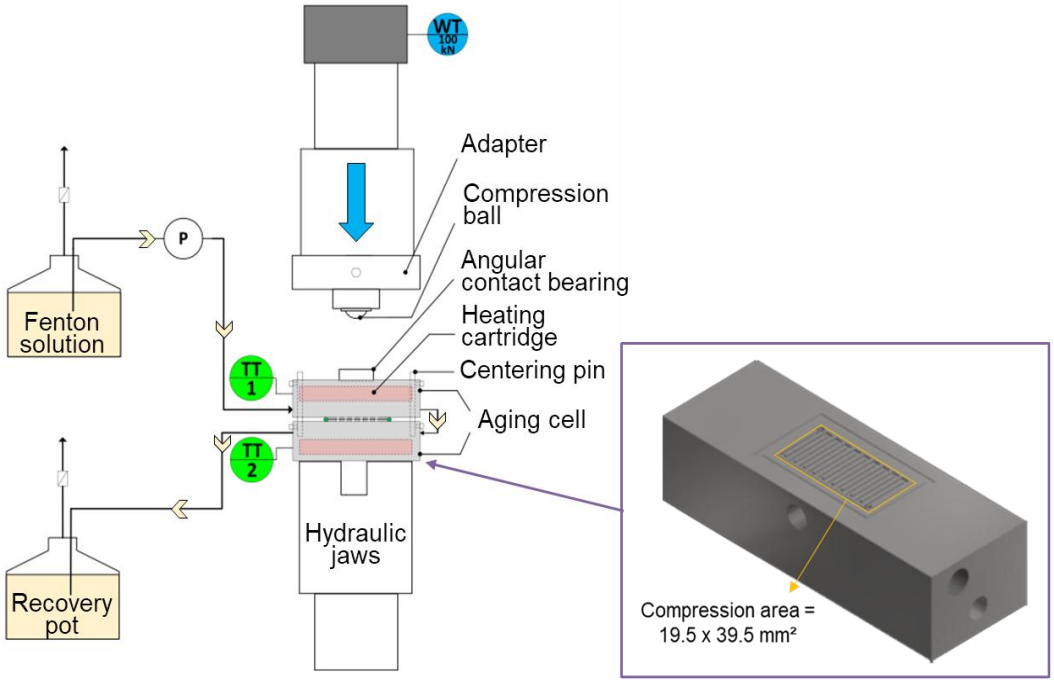

Fig. 1 – Schematic representation of the chemical-mechanical aging device and of the lower part of the aging cell **[39]**. The two symmetric half-cells – or flow field plates – were made in 316L stainless steel because of its excellent mechanical properties (great corrosion resistance and chemical inertness against diluted H_2O_2 solution). Single serpentine channels similar to those used in fuel cells were machined at their surface – with land and channels of 1 mm wide and 0.7 mm deep – to ensure the distribution of the solution on each side of the membrane. The system can accommodate 40– 45 mm wide and 60–70 mm long membrane samples, the area exposed both to the solution and the compressive stress is 19.5 x 39.5 mm² per half-cell.

The mechanical stress exerted on the membrane during fuel cell operation induces a significant increase of local stresses, which could reach up to 10 MPa according to the modelling work of Khattra *et al.* [17]. On the other hand, Kusoglu *et al.* [21] showed that a 5 MPa static compressive stress was sufficient to considerably enhance the chemical decomposition of Nafion™ membranes. Consequently, the force was set to 3610 N and 7220 N, which corresponds to 4.75 and 9.5 MPa for a compression area of about 19.5 x 39.5 mm². For the sake of simplicity, aging tests will be referenced as 5 MPa and 10 MPa thereafter. In addition, since only the channel ribs are in contact with the membrane – their effective area being of about 400 mm² –, it must be kept in mind that the actual pressure applied to the polymer in the absence of gas diffusion layer is rather close to 9 or 18 MPa. The compression area is only used here as a reference, as commonly done with fuel cell active area.

An EPDM (Ethylene Propylene Diene Monomer) O-ring gasket was used to guarantee the aging cell sealing. The cell temperature (80 °C) was regulated thanks to cartridge heaters and

thermocouples introduced into each half-cell, close to the membrane. The half-cells were inserted between the clamps of an electromechanical MTS testing machine (load frame model 312.21). A specific adapter (Fig. 1) was designed to ensure a homogeneous distribution of the pressure – controlled thanks to a pressure measurement film (Prescale Super Low Pressure sheet, Fujifilm) – on the compression area of the membrane during the aging tests. Prior to each aging test, a preliminary measurement aiming at defining the minimal pressure required to press the gasket and guarantee an optimum sealing was performed. This minimal pressure was assumed to correspond to the 0 MPa reference level seen by the membrane.

2.3 Ex-situ coupled mechanical and chemical aging tests

Various tests were carried out to investigate the impact of chemical and mechanical stress on XL and NR211 membranes. The solution flow rate (3.0 $mL.min^{-1}$) and the temperature (80 °C) remained constant for all these tests.

As a first step, preliminary tests were carried out by applying the 0 MPa reference pressure (§2.2) while circulating a 3 vol% H_2O_2 solution (***control aging test #1***) or a Fenton solution containing 3 vol% of H_2O_2 and 1 ppm of ferrous ions Fe^{2+} (***control aging test #2***). All the aging tests consisting in the circulation of Fenton solution were carried out with these concentrations, determined thanks to previous works [39,41].

The second step consisted in applying a cyclic compressive stress of 5 MPa combined with the circulation of degrading solutions for 8 hours: a first experiment (***short-term aging test #1***) was performed with only H_2O_2 to simulate moderately aggressive conditions while a second experiment was performed in more aggressive conditions with a Fenton solution (***short-term aging test #2***).

Additionally, an aging test similar to ***short-term aging test #2*** was performed for 20 hours to study the effect of exposure time. This aging test will be referred to as ***long-term aging test #2*** in the following. Complementary tests were also carried out by coupling the circulation of a Fenton solution and the application of a static 2.5 MPa compressive stress on the one hand (***static aging test***) and a 10 MPa cyclic compressive stress on the other hand (***high pressure aging test***). These tests were believed to provide some information on the effect of stack clamping pressure and high compression level which can be locally experienced by the membrane during fuel cell operation.

Table 1 summarizes the main operating conditions used for the aging tests discussed in this study.

After the tests, the samples were removed from the cell, immersed in distilled water, then soaked in EDTA-Na_2 solution (0.01 $mol.L^{-1}$) at room temperature overnight to remove a possible cationic contamination due to the iron ions used in Fenton solution. After that, the samples were re-acidified in HNO_3 solution (1 $mol.L^{-1}$) at 80 °C for two hours and washed in distilled water at 80 °C for another two hours. They were finally dried in an oven at 60 °C during 20 hours before being analyzed.

Table 1 – Summary of the operating conditions of the *ex-situ* tests coupling mechanical and chemical stresses.

Name of the experiment	Mechanical strength	Chemical conditions	Duration	Number of tests performed
Control aging test #1	Static 0 MPa	H_2O_2 solution	8 hours	2
Control aging test #2	Static 0 MPa	Fenton solution	8 hours	2
Short-term aging test #1	5 MPa cycling	H_2O_2 solution	8 hours	2
Short-term aging test #2	5 MPa cycling	Fenton solution	8 hours	4
Long-term aging test	5 MPa cycling	Fenton solution	20 hours	2
Static aging test	Static 2.5 MPa	Fenton solution	8 hours	2
High pressure aging test	10 MPa cycling	Fenton solution	8 hours	2

2.4 Physico-chemical characterizations

2.4.1 Fluoride ions release

The solutions having circulated through the cell were collected and analyzed to determine the amount of fluoride ions released during the aging tests. The Fluoride Emission Rate (FER) is expressed here in µg of fluoride ions released per gram of dry membrane per hour ($\mu g.g_{Nafion}^{-1}.h^{-1}$). The concentration of fluoride ions released was measured using a pH/millivolt meter (SevenCompact S220, Mettler Toledo) and a fluoride ion-selective electrode (DX219, Mettler Toledo). The electrode was calibrated over the 0.057 – 19 ppm range using various calibration solutions prepared from a commercial standard solution (ISE standard F 1000 ppm, Mettler Toledo).

2.4.2 Characterization of the PFSA chemical structure

To characterize the impact of conjoint chemical and mechanical stress on Nafion™ membranes chemical structure, only the compression area (19.5 x 39.5 mm²) was scrutinized. Aged XL and NR211 membranes were analyzed thanks to ATR-FTIR and solid-state ^{19}F-NMR spectroscopies to investigate the evolution of the chemical structure at the scale of the PFSA repeat unit. The acquisition of ATR-FTIR and solid-state ^{19}F-NMR spectra were carried out following in identical conditions as described in ref. [42].

2.4.3 Characterization of the functional properties of membranes

A dynamic vapor sorption analyzer (IGAsorp, Hiden Isochema) with a mass resolution of about ± 0.2 µg was used to establish the membrane samples' sorption isotherms. To determine the dry mass of the samples, they were first dried at 60 °C under a nitrogen flow rate of 250 $mL.min^{-1}$. Sorption isotherms were recorded at 30 ± 0.1 °C for water activities comprised between 0.05 to 0.95, with an increment of 0.05. 3 to 10 hours were necessary to reach the equilibrium at each step, with a mass variation threshold lower than 1 %.

Liquid-state ^{1}H-NMR spectroscopy was used to study the evolution of the water self-diffusion coefficient. ^{1}H-NMR spectra were acquired at 600.13 MHz using an Avance III 600 WB spectrometer and a 5 mm Diff30 probe (Bruker) with a gradient system delivering a maximum intensity of 1800 G.cm^{-1}. 256 scans were recorded and averaged using a recycle delay of 3 s and a dwell time of 25 µs, at 24 °C. The water-self diffusion coefficient was measured using a Pulsed-Gradient STimulated spin-Echo (PGSTE) sequence with unipolar gradients. The measurements were carried out with a gradient pulse duration δ = 1 ms, a diffusion delay Δ = 6.9 ms and a gradient strength g between 40 and 1000 G.cm^{-1}. The water self-diffusion coefficient was then determined by fitting the signal attenuation as a function of the gradient strength thanks to the Stejskal – Tanner equation [43]. Water self-diffusion coefficient of pristine and aged membrane (2 x 4 cm² samples) were measured for different water contents: some samples were fully immersed in distilled water at room temperature for several hours while others were directly analyzed in dry state, depending on the measurements campaign. In the case of immersed membranes, the hydrated samples were quickly pressed between two layers of absorbent paper once out of water to remove residual droplets, before being rolled and packed into 5 mm airtight NMR tubes. In both cases, the samples were equilibrated at least overnight before being weighted and analyzed. The hydration level of each sample was then adjusted by exposing them to a water-saturated environment or to the ambient atmosphere to increase or decrease the water content, as needed. It is important to note that no discrepancy has been observed in water self-diffusion coefficient evolution as a function of the membrane water content between the two operating modes, *i.e.* whether membrane samples were first hydrated and then dehydrated, or the other way.

2.4.4 Electrochemical tests in single cell

Aged membrane samples were hot-pressed to Gas Diffusion Electrodes (Sigracet SGL 29BCE, Hyplat) to make MEA that were then tested in a single cell with a geometry identical to that of the aging cell (§ 2.2). The assembling protocol and FC operating conditions are described in ref. [39].

2.4.5 Macroscopic and microscopic morphology analysis

To highlight the membranes defects, their surfaces were observed using a three-dimensional measurement apparatus: MICROVU Vertex410. This machine was used as an optical microscope in coupling reflection and transmission modes. Lighting in reflection mode, composed of light emitting diodes, was employed at 30 % of its maximum capacity (32 W) and lighting in transmission mode was adjusted at 20 % of its maximum capacity. Each 640 x 480 pixels image was taken at a x21 magnification (*i.e.* 8.78 x 6.59 mm²), at (23 ± 1) °C and (50 ± 5) %RH. 24 images were required to carefully reconstruct the samples area. The *X* and *Y* position of the machine was controlled with a motorized table, while the *Z* axis was slightly varied to optimize the sharpness. The whole set was finally assembled using the *ImageJ* software.

In addition, aged membranes used to make MEA were analyzed by Scanning Electron Microscopy (SEM) after the electrochemical tests in single cell. For comparison, pristine NR211 and XL membranes – pretreated following the protocol described in section 2.1 – were also assembled with Gas Diffusion Electrodes (GDE) and analyzed by SEM, as references for the pristine state. SEM images of fresh/aged MEA cross-sections were acquired with a Field Emission Gun–Scanning Electron Microscopy (FEG–SEM, Zeiss Gemini 500 microscope) to monitor morphological variations of the Nafion™ membranes upon the different aging tests. For the preparation of the cross-sections, the MEA were first embedded in Epoxy® resin, dried under ambient air for 1 day, polished using SiC polishing disk with small grain size (4000) and finally covered by a thin carbon film.

3. Results

3.1 Membranes changes after conjoint mechanical and chemical stress

3.1.1 Fluoride Emission Rates

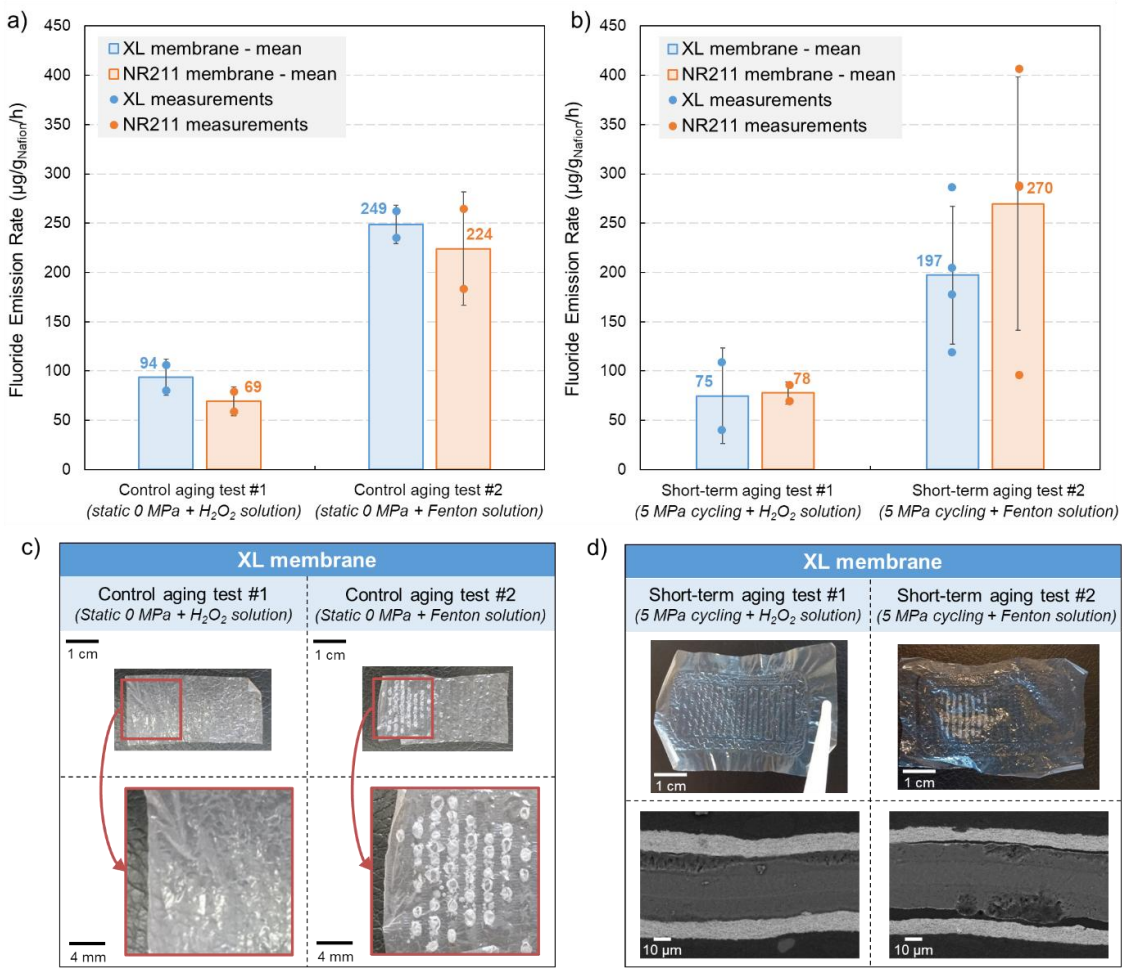

Fig. 2 – Fluoride emission rates (FER) of Nafion™ XL and NR211 membranes under (a) static 0 MPa and (b) cyclic 5 MPa compressive stress coupled to moderate (H_2O_2 solution) and aggressive (Fenton solution) chemical stress. FER presented in Figure 2b correspond to data already published in a previous work **[39]** that have been corrected in this study by subtracting a parasitic contribution in fluoride concentration coming from the TISAB II solution employed for measurements. (c) and (d) illustrate the evolution of the XL membrane morphology at

different scales after the various aging tests. It is noteworthy that SEM images were not acquired in specific area (*i*.e. in the bubbles area) but taken randomly through the membranes cross-section.

Control aging test #1 and ***control aging test #2*** (Table 1) were carried out to define reference levels of fluoride emission rate (FER) after chemical stress exposure, without significant mechanical pressure. A periodic sampling of the solution was performed during the aging tests in order to evaluate the evolution of fluorine concentration as a function of exposure time: unfortunately, it was below the detection limit of our electrode, thus only the time-average value can be discussed. The trend was similar for both membranes, with FER 2.5 to 3.5 times higher when exposed to the Fenton solution than with hydrogen peroxide (Fig. 2a). This trend was already observed in a previous work for aging tests coupling a cyclic compression of 5 MPa and the circulation of H_2O_2 or Fenton solutions (Fig. 2b) as well as in the case of *ex-situ* chemical degradation [39]. Higher degradation rates in Fenton solution than in H_2O_2 solution were expected since the H_2O_2 decomposition and thus the formation of radicals is enhanced/catalyzed by the addition of iron ions, whatever the mechanical stress applied.

The FER of XL membranes under 5 MPa cycling are about 20 % lower than without mechanical stress for both ***control aging test #1*** (H_2O_2 solution) and ***control aging test #2*** (Fenton solution). Conversely, no significant variation of the FER can be observed with NR211 membranes, even though no definitive conclusion can be drawn due to the large error bars. Moreover, the appearance of bubbles and blisters was observed at the membrane surface (Fig. 2c) as well as in the cross-section (Fig. 2d) in the case of XL whereas no such evolution was detected with NR211. This point will be discussed in section 3.1.2.

Table 2 shows the fluoride emissions as functions of the exposure time (20 hours *vs.* 8 hours) for both XL and NR211 membranes in the case of aging tests associating 5 MPa cyclic pressure and Fenton solution (mentioned as ***long-term aging test*** *vs.* ***short-term aging test #2*** in Table 1). Fluoride emissions vary non-linearly with time: much more ions are emitted between 8 and 20 hours than between 0 and 8 hours for both membranes. This suggests an increase of the degradation rates throughout the testing period. It can also be observed that the FER of XL membranes during the 8-20h period approaches that of NR211, despite the presence of supplementary radical scavengers and a reinforcement layer, while it was significantly lower during the 0-8h period. This could indicate that the reinforcement layer and/or radical scavengers no longer allow to limit or slow down the polymer decomposition once a certain level of mechanical stress is reached.

Table 2 – Fluoride emission rates of XL and NR211 membranes after short-term and long-term aging tests

	XL membrane		**NR211 membrane**	
	0-8h solution	**8-20h solution**	**0-8h solution**	**8-20h solution**
Fluoride emission rate ($\mu g.g_{Nafion}^{-1}.h^{-1}$)	197 ± 70	668 ± 42	270 ± 129	623 ± 7

The comparison of the mechanical stress applied to a membrane (*i.e.* static at 0 or 2.5 MPa, 5 or 10 MPa cycling) simultaneously exposed to a Fenton solution shows two distinct behaviors: on the one hand, the FER of NR211 does not seem to be greatly affected, with values comprised between 224 and 324 $\mu g.g_{Nafion}^{-1}.h^{-1}$ (Fig. 3). On the other hand, the behavior of XL membrane is different: doubling the mechanical strength (***high pressure aging test*** *vs.* ***short-term aging test #2*** in Table 1) leads to a significant increase of the FER, *i.e.* from 197 to 316 $\mu g.g_{Nafion}^{-1}.h^{-1}$. In addition, the FER of XL membrane with no or negligible mechanical pressure (*i.e.* 0 MPa) is strikingly high compared to more severe solicitations. This result cannot be simply explained in the view of our current results and deserve further investigations to shed light on this singular behavior.

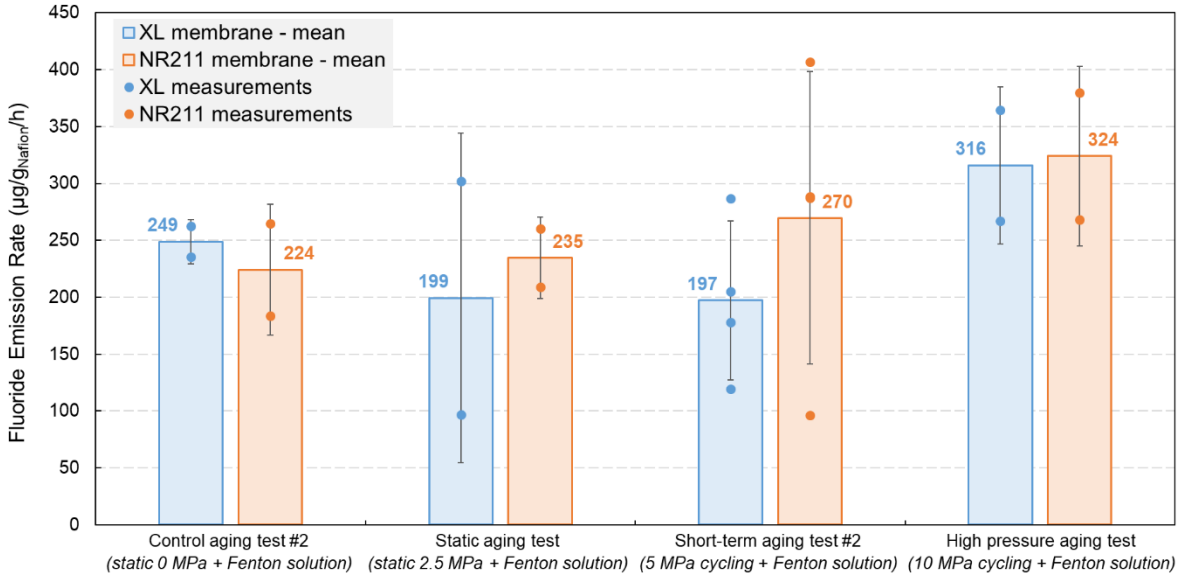

Fig. 3 – Fluoride emission rates (FER) of Nafion™ XL and NR211 membranes under various mechanical stress coupled to the Fenton solution exposure.

The slightly better behavior of XL membranes *vs.* NR211 – in terms of FER – may be explained by the presence of a reinforcement layer [26,36]. The improved mechanical durability of XL membranes was already discussed in the literature and could be due to a higher strength and toughness as well as a better resistance to creep and fatigue [44–48]. One can also imagine that when mechanical stress becomes too high, the reinforcement layer of XL membrane does no longer impede polymer decomposition, so that FER reach similar orders of magnitude as non-reinforced NR211 membrane. Furthermore, XL membrane also contains radical scavengers – as opposed to NR211 membrane – which contributes to prevent chemical degradation by radical attacks on polymer chains: their positive impact may be less significant after long-term aging. In the view of our current results, the respective contributions of the mechanical reinforcement layer and radical scavengers cannot be discriminated.

3.1.2 Morphological modifications at macroscopic and microscopic scales

Short-term aging test #2 and ***control aging test #2*** led to the appearance of tiny localized bubbles close to the surface of XL membranes, mostly in the channels area: *i.e.* where the membranes were in direct contact with the Fenton solution but without mechanical stress (Fig. 2c). On the contrary, such defects are not observed with NR211, neither to the naked eye nor with a stereo microscope, regardless of the conditions. Although the image presented in Fig. 2c show bubbles and blisters localized on one side of the membrane, abundance of bubbles in this area was not systematically found in the reproducibility tests: we can see in Fig. 4 that this phenomenon is not observed. In the view of all tests performed, there does not seem to be preferential localization area(s) for the bubbles, apart from the channel/land discrepancy. Note that the appearance of such morphological changes in regions that are not directly subjected to mechanical stress (the channels) may suggest the existence of indirect degradation mechanisms.

Such defects have already been observed in the case of pure chemical exposure to Fenton solutions but in harsher conditions (higher H_2O_2 and ferrous ions concentration) for both reinforced [19,39] and non-reinforced membranes [39,49–53]. This may indicate that additional mechanical stress (static or cyclic compression) could induce more severe morphological changes than the exposure to Fenton solution only. However, the conditions in which the chemical stress is applied in these studies are not directly comparable: *i.e.* membranes were immersed in a static solution in one case *vs.* a fresh and flowing solution in the other case. Furthermore, it is worth noting that such morphological changes have never been reported after fuel cell operation (neither regular operation nor accelerated stress tests).

SEM analysis allows to investigate the impact of conjoint chemical and mechanical stress on XL membrane morphology at the microscopic level. In the case of ***short-term aging tests #1*** and ***#2*** (Fig. 2d), and contrary to the observations made at the macroscopic scale, localized deformations are observed in the external PFSA layers of the XL membrane, even with an H_2O_2 solution. The exposure to a Fenton solution appears to exacerbate theses morphological changes while the central PTFE-rich reinforcement layer does not seem altered, neither with H_2O_2 nor with the Fenton solution. However, it is worth noting that no clear correlation can be established between the observation of bubbles and blisters at the macroscopic level and the presence of localized deformations at the microscopic level.

Further investigations were carried out to study the impact of more severe solicitations – *i.e.* up to 10 MPa or during 20 hours of aging (***high pressure aging test*** and ***long-term aging test***, respectively) – on the XL membrane morphology. Exposing the XL membrane simultaneously to cyclic 10 MPa compression and Fenton solution (***high pressure aging test***) led, as previously observed, to the appearance of many tiny bubbles and blisters, in the channel area, and close to the membrane surface (Fig. 4).

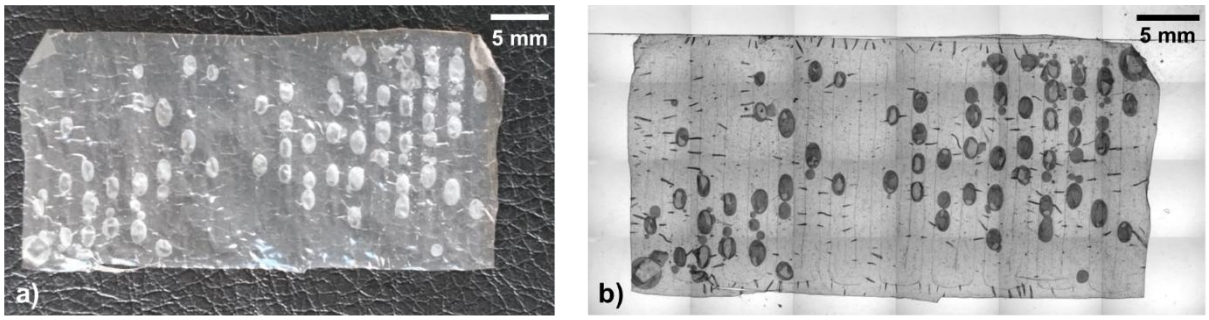

Fig. 4 –Top view analysis of the bubbles and blisters formed at the Nafion™ XL membrane surface (a) to the naked eye and (b) using the non-contact MicroVu device.

When the duration of the 5 MPa cycling and Fenton exposure test was extended from 8 to 20 hours (***long-term aging test)***, the fluoride emissions increased considerably (§ 3.1.1 and Table 2) – indicating an acceleration of the degradation – and became similar for both NR211 and XL membranes. The higher FER measured with XL after 20 hours is consistent with the more significant morphological changes observed (Fig. 5a): many bubbles and blisters were present close to the XL membrane surface with an inhomogeneous distribution along the channel area. At the microscopic level, SEM analyses of the cross-sectional microstructure of XL membrane (Fig. 5c) also revealed many local defects close to the membrane surface, which is consistent with the strong morphological changes already observed to the naked eye (Fig. 5a). Additionally, SEM images show the appearance of some cracks at the interface between the external PFSA layer and the central PTFE-rich reinforcement layer, as well as into the external PFSA layer: when they appear at the interface, those cracks may be considered as the beginning of a delamination process, although this was not directly observable to the naked eye.

Conversely to XL membrane, and similarly to the observations made for ***short-term aging test #2*** and ***control aging test #2***, no morphological changes were observed to the naked eye for the NR211 membrane, whether the mechanical solicitation was increased to 10 MPa or the duration extended to 20 hours (Fig. 5d). However, SEM images showed a "foamy" structure through the entire NR211 thickness, accompanied by the formation micron-sized holes within the membrane.

Although the chemical-mechanical stress on XL and non-reinforced NR211 membranes is strictly identical, the resulting morphological changes differ: unlike NR211 membrane, XL membrane does not have a foam-like appearance through its whole thickness but local defects close its surface, as well as microcracks along the PTFE/PFSA interface.

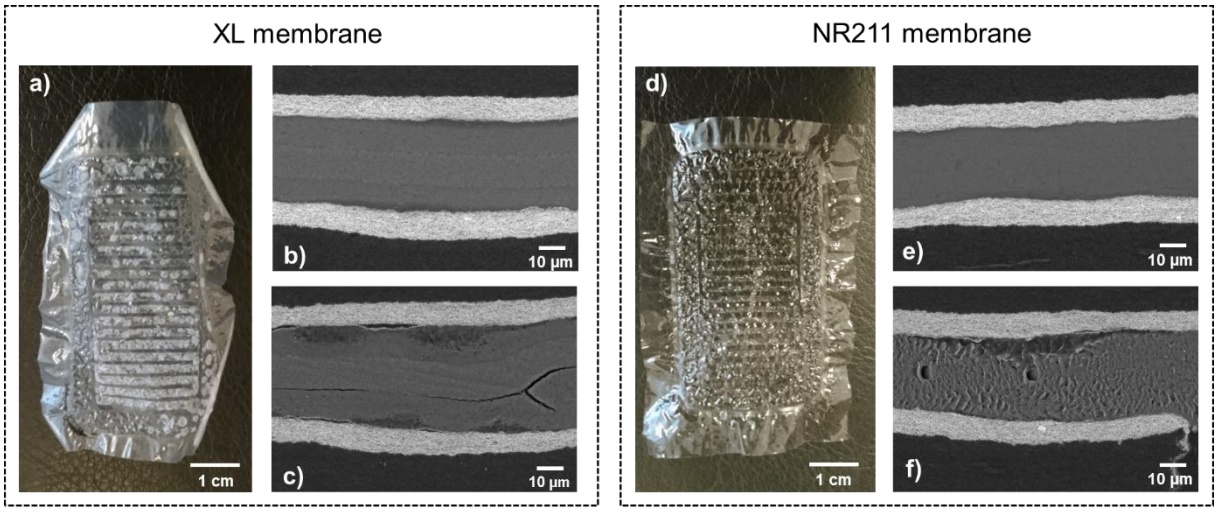

Fig. 5 – Macroscopic surface morphology of Nafion™ (a) XL and (d) NR211 membranes after ***long-term aging test*** and comparison of SEM cross-sections for pristine and aged (b, c) XL and (e, f) NR211 membranes. SEM images were performed on MEA made with aged membranes and after conducting the electrochemical tests in single cell (more details are given in section 2.4.5).

To the best of our knowledge, no such interfacial delamination of the XL membrane has been reported in the literature after neither *in-situ* fuel cell operation nor *ex-situ* aging protocols. Nonetheless, Zhang *et al.* recently showed that during fatigue experiments, cracks were initiated and propagated in external PFSA layers without affecting the PTFE reinforcement layer, while delamination occurred at the interface between external PFSA and PTFE reinforcement layers [48]. They suggested that the presence of delamination between the different layers helps to alleviate the stress experienced by the membrane by transferring the mechanical stress through the bridging PTFE fibers: there is indeed no evidence of a decrease of the membrane/fuel cell performance due to such delamination. Furthermore, Shi *et al.* recently showed that crack propagation mechanisms were identical with pristine and chemically aged XL membrane, *i.e.* crack growth in external layers and interfacial delamination [19]. In the present study, the cyclic 5 MPa compressive stress may have led to interfacial delamination like those observed in the literature.

3.1.3 PFSA chemical structure

Solid-state ^{19}F-NMR spectroscopy analyses were performed after ***short-term aging tests #1*** and ***#2***. The NMR spectra are displayed in Fig. S1 of Supplementary Information (SI). The resonance peaks of Nafion™ and the predicted peak areas have already been identified and assigned in the literature [54–56]. In addition, several works established a relationship between the number of moles of tetrafluoroethylene (TFE) per moles of comonomer unit and the integral of the resonance peaks associated to the PFSA chain fragments, thus permitting to determine the ion-exchange capacity (IEC) [38,57] (Table 3). The experimental values determined for pristine XL and NR211 membranes are in good agreement with the supplier datasheet and literature values [57,58]**.**

Table 3 – Experimental values of the Ion-Exchange Capacity (IEC) deduced from the NMR spectra for XL and NR211 membranes after ***short-term aging tests #1*** and ***#2*** in comparison with pristine membranes.

	Pristine membrane		Short-term aging test #1 (H_2O_2)		Short-term aging test #2 (Fenton)	
	XL	**NR211**	**XL**	**NR211**	**XL**	**NR211**
Ion-Exchange Capacity (meq.g^{-1})	0.90 ± 0.02	0.99 ± 0.02	0.90 ± 0.02	1.01 ± 0.02	0.90 ± 0.02	1.01 ± 0.02

Regardless of the degrading solutions, no significant evolution of the intensity of the side chain resonance peaks (Fig. S1) or of the IEC (Table 3) are observed for both membranes. This indicates that the global membrane degradation does not seem to affect the PFSA chemical structure. This observation matches those made after an *ex-situ* chemical stress induced by Fenton's reaction in a previous work [42], with:

- a constant intensity ratio between the side chain and the CF_2 groups,
- no significant IEC change,
- but still significant fluoride emissions in the solution.

This leads the conclusion that the polymer decomposition occurs most probably in similar proportion for both main and side chains. Since solid-state ^{19}F-NMR spectroscopy only permits to analyze the global chemical structure of aged membranes, ATR-FTIR spectroscopy was also employed to analyze the evolution of the PFSA chemical structure close to the surface, thus excluding the PTFE reinforcement of XL membrane. No significant variation of the relative intensity of side chain vibration bands are visible in the IR spectra for both membranes and regardless of the aging test performed. These results are consistent with the conclusion made after the NMR measurements: ATR-FTIR and NMR spectroscopies both suggest that conjoint chemical and mechanical stresses do not significantly alter the chemical structure of the PFSA repeat unit.

3.2 *Impact of conjoint mechanical and chemical stress on the functional properties and cell performances*

3.2.1 Water sorption capacity

Fig. 6 illustrates the evolution of water sorption isotherms as well as those of the adsorption mechanisms in XL and NR211 membranes. The results of all tests performed (Table 1) are shown in Fig. 6, with the exception of the ***long-term aging tests*** for which aged membranes were assembled with GDE in order to detect possible hydrogen permeation and evaluate their cell performances. In the case of XL membranes, similar behaviors are observed in all cases: the sorption isotherms differ from that of the pristine membrane by a significant increase of the cluster contribution after degradation. A hygrothermal test, consisting in immersing the XL membrane in deionized water at 80°C for 24 hours (Fig. S2), was performed and led to an identical increase of the cluster contribution. This phenomenon has also been observed by Shi *et al.* [59] for pre-heated XL membranes (*i.e.* pristine XL heated in deionized water at 70 °C for one hour prior to sorption measurement) and, as stated by the authors, it can be attributed

to nanostructural changes bringing the membrane closer to its quasi-equilibrium state as a consequence of high temperature. In our case, it can be therefore concluded that this behavior does not result from the degradation induced by chemical or chemical-mechanical solicitation.

As a reminder, the cluster contribution corresponds to the aggregation of water molecules in the pores of the membrane at high water activities, resulting in its macroscopic swelling. On the contrary, Langmuir and Henry contributions – describing the solvation and further hydration shells formed around sulfonate groups – do not seem to be affected, even though FER can be highly different from one case to the other, *i.e.* between static 2.5 MPa and cyclic 10 MPa, for example.

With NR211 membranes, the sorption isotherms do not seem greatly impacted over the whole water activity domain. This is consistent with the absence of significant changes in the ^{19}F-NMR spectra or IEC discussed in section 3.1.3. These results are in agreement with those obtained in a previous work, when membranes were exposed to purely chemical stress tests [42]: this suggests that the severe additional mechanical stress experienced by the membranes has no significant impact on the water sorption capacity of Nafion™ membranes. This assumption is also supported by the absence of significant evolution of the FER with NR211 membranes exposed to a static or cyclic compressive stress of 0, 2.5, 5 or 10 MPa (Fig. 3).

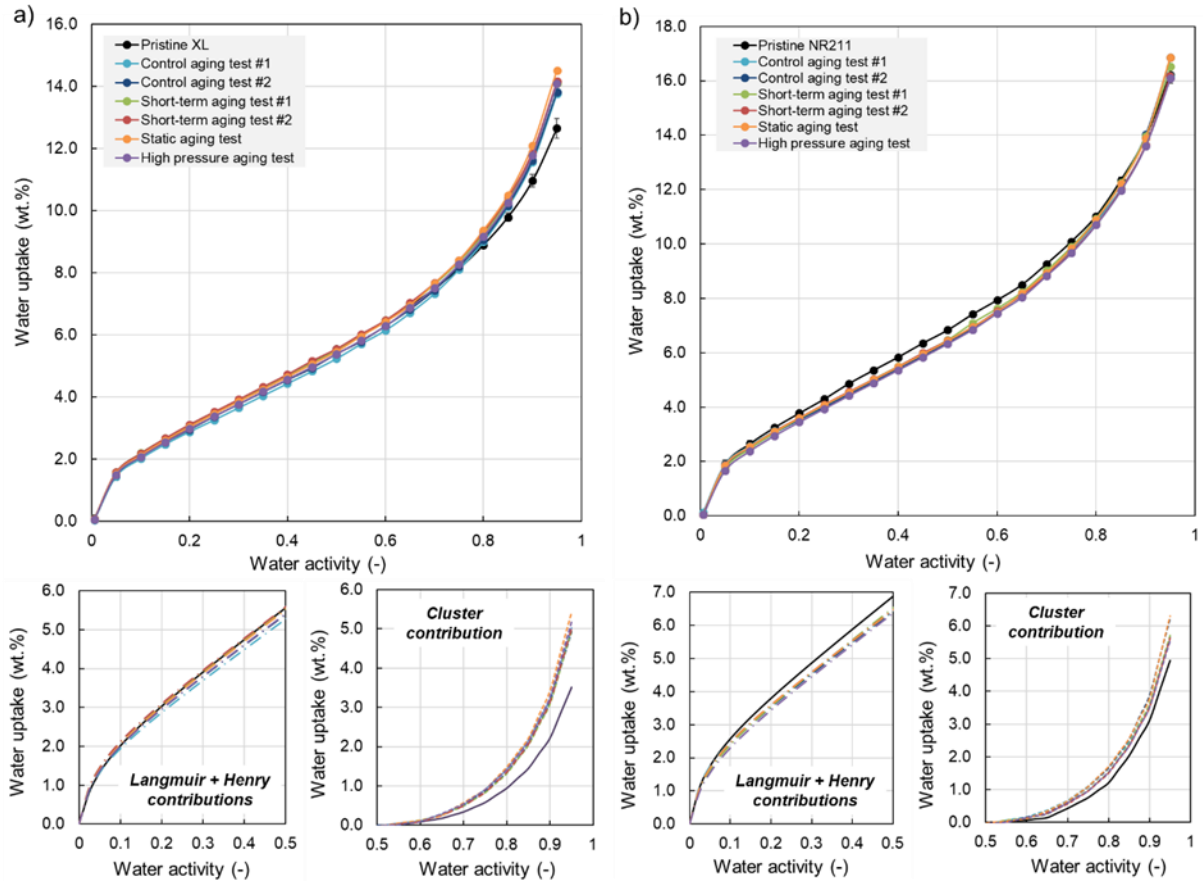

Fig. 6 – Water sorption isotherms (30 °C) of (a) XL and (b) NR211 membranes after various aging tests in comparison with pristine membranes. The plots at the bottom illustrate the evolution of the different adsorption mechanisms for XL (to the left) and NR211 (to the right) membranes. Five measurements were performed on the pristine XL to control the repeatability of the measurement and of the pretreatment process. The water sorption isotherms of pristine XL and NR211 membranes have been already published in a previous work **[42]**.

3.2.2 Water self-diffusion coefficient

Water transport property was investigated by liquid-state ^{1}H-NMR spectroscopy. Fig. 7 illustrates the evolution of water self-diffusion coefficient in XL and NR211 membranes as functions of the water uptake after various aging tests: no significant variation is observed over the whole range of water-uptake probed, whether the membranes were exposed to static or cyclic compressive stress. However, the values obtained with aged XL and NR211 membranes are generally very close to the lower limit of those measured with pristine samples, which may suggest that the mechanical-chemical aging involved in our conditions has no significant impact on water self-diffusion property. Again, this trend has already been observed in the case of membranes submitted to a chemical stress only [42]. This shows that the introduction of an additional mechanical stress does not affect the water diffusion behavior of membranes, whether they are reinforced or not.

In the light of these results, it can be concluded that the addition of a mechanical stress to a chemical stress increases significantly the FER (§ 3.1.1) but does not alter further the Nafion™ membranes chemical structure (repeat unit, IEC) and functional properties (water sorption and self-diffusion). However, due to the presence of the flow-field plates, the membrane surface has not been exposed to identical mechanical and chemical stresses under the lands and under the channels. It can thus be argued that the polymer decomposition may be heterogeneous. As the measurements made in this work only reflect the overall degradation of Nafion™ membranes, characterizing separately PFSA chemical structure and properties with a localized approach would help to discriminate the degradation behaviors between regions located under the lands and under the channels.

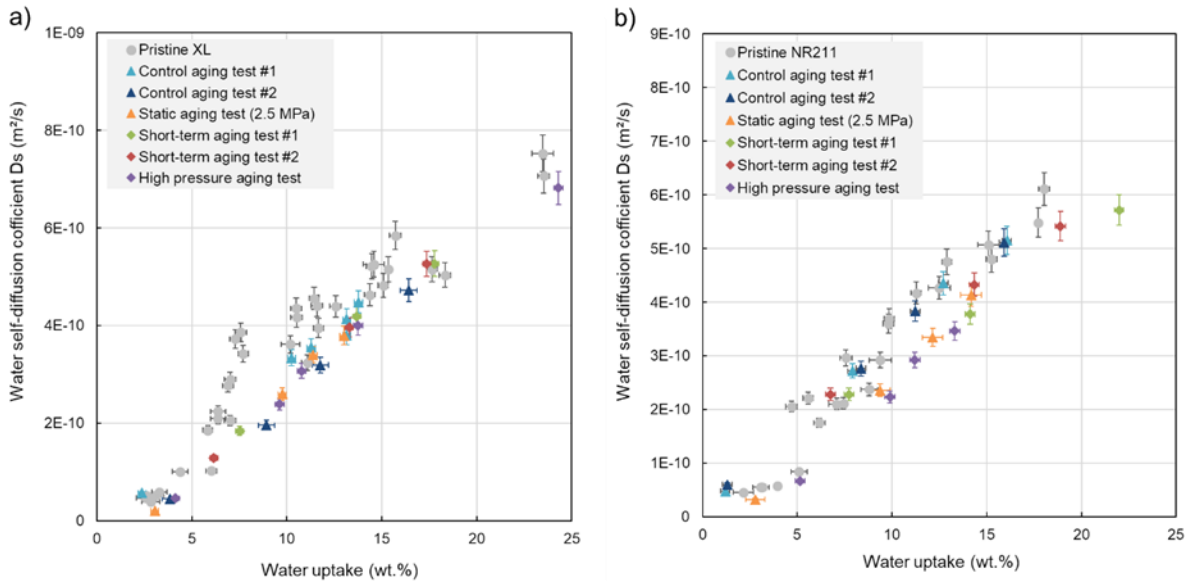

Fig. 7 – Water self-diffusion coefficient evolution after various aging tests as a function of water uptake in (a) XL and (b) NR211 membranes (diamond symbols for static compression and triangle symbols for cyclic compression) in comparison with pristine membranes (circles).

3.2.3 Fuel cell performances

Finally, some aged membranes were used to make MEA and tested in a single cell to evaluate their functional properties and detect possible hydrogen leaks. The results obtained in the case

of ***short-term aging test #2*** has been already presented in a previous work [39] and only XL and NR211 membranes submitted to the ***long-term aging test*** have been tested in the present study. Table 4 displays the permeation current, high frequency resistance and Open Circuit Voltage (OCV) measured for the aged membranes in comparison with the values obtained for pristine ones. As observed in our previous work for the ***short-term aging test #2***, no significant permeation current measured. Only a slight increase of the high frequency resistance is observed for both membranes, which could indicate a slight loss of the proton conductivity because of the membrane degradation. Such a behavior was not expected in light of the considerable morphological changes in XL membranes (§ 3.1.2). Nonetheless, it may be possible that the MEA hot-pressing process led to the closing of some of the blisters near to the membrane surface. In any case, the low hydrogen permeation currents clearly mean that, in this case, none of the blisters led to a membrane failure.

As a complement, polarization curves were also measured with aged XL and NR211 membranes (Fig. S3) and a trend similar to that reported in our previous work for ***short-term aging test #2*** was observed [39] *i.e.* no significant change is perceptible in the case of aged NR211 while only a slight increase of resistive losses is detected for aged XL membrane. As previously proposed in ref. [39], it might be possible that this increase of resistive losses was at least partly related to the modification of the membrane surface, making it difficult to ensure a good electrical contact with the electrodes.

Table 4 – Characterization parameters of cell performances for Nafion™ XL and NR211 membranes exposed to cyclic 5 MPa compression and Fenton solution for 8 and 20 hours in comparison with pristine membranes.

	Pristine membrane		**Short-term aging test #2**		**Long-term aging test**	
	XL	**NR211**	**XL**	**NR211**	**XL**	**NR211**
Permeation current ($mA.cm^{-2}$)	1.80 ± 1.11	1.94 ± 0.75	1.68 ± 0.26	2.54 ± 0.20	1.16 ± 0.05	1.29 ± 0.07
High Frequency Resistance ($m\Omega.cm^{-2}$)	78.7 ± 10.8	67.9 ± 2.7	107.1 ± 5.2	72.7 ± 5.7	113.4 ± 3.8	82.6 ± 2.3
Open Circuit Voltage (V)	0.917 ± 0.018	0.907 ± 0.017	0.906 ± 0.006	0.895 ± 0.004	0.922 ± 0.004	0.920 ± 0.005

4. Discussions

4.1 Comparison with ex-situ chemical stress test

The changes in water sorption properties of the composite Nafion™ XL membrane after mechanical-chemical aging tests is compared to that of a purely *ex-situ* chemical stress test in Fig. 8. The trends are similar without any significant change except for a slight increase of the cluster contribution in both cases, a phenomenon already described and attributed to a thermal effect by Shi *et al.* [59] (§ 3.2.1). This indicates that the water sorption of XL membrane is

not greatly affected by the exposure to coupled mechanical and chemical stress. In a recent study [42], we suggested that the addition of a mechanical fatigue to a chemical stress would lead to solicitations and degradation mechanisms closer to those occurring during fuel cell operation. In this work, however, it seems that combining a rather important compressive stress with a chemical stress does not significantly alter Nafion™ degradation mechanisms, nor its functional properties (water sorption capacity and self-diffusion coefficient). This conclusion is supported by some results of this study (*e.g.* increasing the cyclic pressure applied to NR211 membrane from 0 to 5 or 10 MPa during 8 hours has no impact on fluoride emissions), which is in agreement with our previous results [42]. Nonetheless, this conclusion is not consistent with the results of Kusoglu *et al.* [21], who observed an increase of polymer degradation by applying a static pressure to the membrane. However, their work was performed in conditions significantly different from ours:

- They used a thicker Nafion™ 117 membrane (178 µm) previously exchanged with ferrous ions Fe^{2+} and a 6 vol% H_2O_2 solution *vs*. 3 vol% H_2O_2 concentration in our case,
- Contrary to the present work, the stress cell designed by Kusoglu *et al.* did not contain single serpentine flow channel, implying a homogenous exposure of the mechanical stress.

Despite these *a priori* more aggressive conditions, they observed degradation rates more than 50 times lower than ours, so that their results and ours are not easily comparable. Finally, we imposed a cyclic compressive stress while Kusoglu *et al.* maintained a static compressive stress during several days (*i.e.* 7 days in total). However, the combination of cyclic compression and Fenton exposure, as studied in the present work should be considered as a rather severe solicitation (§ 2.2) and we can only notice that it has a mild impact on the degradation.

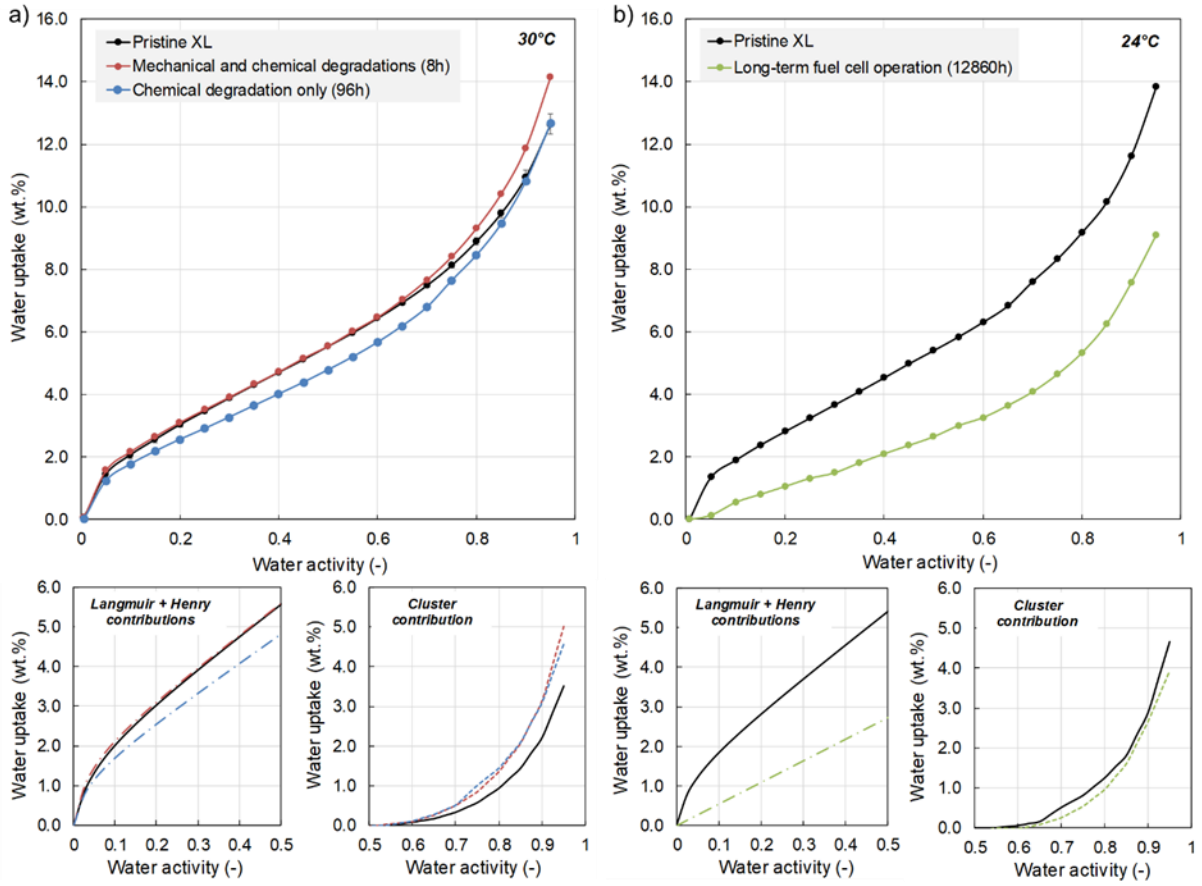

Fig. 8 – Evolution of water sorption isotherms in XL membranes (a) after *ex-situ* conjoint degradation (***short-term aging test #2***) and after *ex-situ* chemical degradation only (Fenton solution exposure) in comparison with the evolution (b) after long-time fuel cell operation **[38]**.

4.2 Comparison with fuel cell operation

To this point, it may be worth comparing the evolutions of water sorption isotherms after *ex-situ* stress tests with those measured after long-time fuel cell operation (Fig. 8) in a previous work [38]: the cluster contribution was not impacted while the Langmuir contribution was strongly reduced. This trend was attributed to a significant IEC reduction, because of a partial loss of sulfonic groups, which differs considerably from that observed after the present *ex-situ* stress tests, with fairly unaltered functional properties. However, measurements performed after FC operation were focused on specific areas [37] – inlet/outlet of reactant gases – that were visually degraded and known to be exposed to severe conditions: high hydrogen crossover [60,61], low relative humidity [62,63] and air starvation [64]. Moreover, the membranes are – mostly, at least – exposed to a gaseous environment in FC systems which differs significantly from the conditions involved in this study, the membranes being in direct contact with aqueous solutions. This may be representative of the conditions experienced by some specific areas submitted to water flooding during FC operation [57,65]. In this regard, the most probable explanation for the discrepancy between the degradation of XL membranes observed after long-time fuel cell operation [38] and those we observe in this work would lie mostly in the difference of operating conditions/time scales or in the nature of the chemical stress – with possibly chemical conditions that were not aggressive enough to have significant

impacts on Nafion™ membrane functional properties – despite the clear chemical degradation evidenced in a previous work [42].

Ex-situ accelerated stress tests are useful to decorrelate the various stressors and aging mechanisms occurring during fuel cell operation. In this work, although a significant increase of FER was observed with the stress level, no thinning and no full-thickness cracks – through the measurement of hydrogen permeation current and SEM images – were observed in the membrane, which differs from the failure modes reported in the case of *in-situ* COCV AST [23,26–28]. Additionally, we noticed the appearance of bubbles and blisters for XL membrane whereas this phenomenon has never been observed – or at least reported – in the literature after FC operation. Since this study only focused on one type of conjoint stress experienced by membrane during operation, it is conceivable that our *ex-situ* stress tests (chemical or mechanical + chemical) do not accurately replicate the more complex chemical conditions encountered by the membranes in actual PEMFC. More particularly, these results can suggest that the use of humidified gases during FC operation and/or the presence of the other FC components – and of the interface between them and the membrane – play an important role on the degradation mechanisms. Nevertheless, it must be kept in mind that the FER values measured in this work were significantly lower than those reported for *in-situ* COCV AST [23,24]. Therefore, modifying the operating procedure by exposing the membrane to a Fenton's environment with gaseous H_2O_2 instead of aqueous solution or introducing Gas Diffusion Layers (GDLs) between the membrane and the flow field plates are natural perspectives to this work, to better mimic FC operating conditions.

5. Conclusions

This study aimed to investigate the impact of coupled mechanical and chemical stress on Nafion™ membranes through an *ex-situ* approach. In that respect, a custom-made device able to reproduce conditions close to that experienced by the membranes during FC operation was developed. Accelerated aging tests were performed to provide some understandings on the influence of mechanical stress – either static or cyclic with varying pressure – on the chemical degradation of Nafion™ membranes, and its impact on their chemical structure and functional properties. As a general conclusion, and from a qualitative point of view, the membranes response to a chemical stress was similar when static or cyclic mechanical stress was added: more severe degradations were observed after Fenton exposure, compared to H_2O_2, both from chemical and morphological points of view. Despite evidence of chemical decomposition and of morphological evolution, aged XL and NR211 membranes did not fail after chemical-mechanical *ex-situ* aging tests – and this regardless of the stress level imposed – since their functional properties were maintained and their fuel cell performances still satisfactory. In addition, the results permitted to highlight the following points:

- Although Fenton's reagent concentrations were low to be as close as possible to real fuel cell operating conditions – *i.e*. without inducing drastic morphological changes – the combination of mechanical stress and Fenton solution exposure led to the

appearance of bubbles and blisters in the case of aged XL membranes. Conversely, no such morphological modifications were observed for NR211 membranes.

- Higher fluoride emission rates were generally obtained with NR211 than with XL. The PTFE reinforcement layer, providing better mechanical strength and dimensional stability to XL membranes [21,25], can explain its better behavior against conjoint degradation. The higher resistance of XL was confirmed by the absence of significant increase in the hydrogen permeation current after the stress tests. Moreover, an increase of FER with the applied pressure was observed in the case of XL for cyclic compression while mechanical stress had no significant impact on the chemical degradation of NR211.
- Long-term aging tests demonstrated that membranes are strongly affected, both from chemical – through the fluoride emission rates – and morphological points of view. SEM analysis revealed that the degradation behavior differs between a reinforced membrane and a non-reinforced one: local deformations and delamination at the interface between PFSA external layer and PTFE-rich reinforcement layer were observed in the case of aged XL while a more homogenous morphology alteration with a foam-like appearance was observed for NR211.
- Despite sometimes severe morphological changes, and rather paradoxically, no changes in the chemical structure or in the water sorption and transport properties of both NR211 and XL Nafion™ membranes were observed.
- Finally, and in agreement with our previous results [39], adding important compressive stress to a chemical stress did not strongly modify Nafion™ membranes FER nor their functional properties, suggesting that even though mechanical stress had an impact, the degradation mechanisms remained – in our case – mostly governed by chemical stress.

The custom-made device and the associated accelerated aging tests developed for the present study constitutes a first step towards a better understanding on chemical and mechanical degradations phenomena of PFSA membranes and open a large variety of perspectives. For instance, one can imagine extending the experiment duration to several tens of hours to deeply challenge the mechanical durability of the membranes. On the other hand, supplementary investigations and reproducibility tests are needed to understand the morphological changes experienced by the reinforced membranes, and more particularly the origin and location of bubbles and blisters formed during conjoint stress tests. Furthermore, performing more localized analysis of aged membranes would help to clarify the contribution of the mechanical stress on membrane chemical degradation as well as the impact of conjoint stress on the chemical structure and functional properties of Nafion™ membranes. Finally, the mechanical stress resulting from humidity cycling in FC may also be of tensile-compressive nature, and it may be worth developing a new experimental set-up able to mimic such stress, coupled with chemical attacks.

Acknowledgements

The authors would like to acknowledge Pr. Stéphane André for the access to the electromechanical universal testing machine.

References

[1] R. Borup, J. Meyers, B. Pivovar, Y.S. Kim, R. Mukundan, N. Garland, D. Myers, M. Wilson, F. Garzon, D. Wood, P. Zelenay, K. More, K. Stroh, T. Zawodzinski, J. Boncella, J.E. McGrath, M. Inaba, K. Miyatake, M. Hori, K. Ota, Z. Ogumi, S. Miyata, A. Nishikata, Z. Siroma, Y. Uchimoto, K. Yasuda, K. Kimijima, N. Iwashita, Scientific aspects of polymer electrolyte fuel cell durability and degradation, Chem. Rev. 107 (2007) 3904–3951. https://doi.org/10.1021/cr050182l.

[2] L. Dubau, L. Castanheira, F. Maillard, M. Chatenet, O. Lottin, G. Maranzana, J. Dillet, A. Lamibrac, J.-C. Perrin, E. Moukheiber, A. ElKaddouri, G. De Moor, C. Bas, L. Flandin, N. Caque, A review of PEM fuel cell durability: materials degradation, local heterogeneities of aging and possible mitigation strategies, Wiley Interdiscip. Rev. Energy Environ. 3 (2014) 540–560. https://doi.org/10.1002/wene.113.

[3] J. Zhao, X. Li, A review of polymer electrolyte membrane fuel cell durability for vehicular applications: Degradation modes and experimental techniques, Energy Conversion and Management. 199 (2019) 112022. https://doi.org/10.1016/j.enconman.2019.112022.

[4] M. Zatoń, J. Rozière, D.J. Jones, Current understanding of chemical degradation mechanisms of perfluorosulfonic acid membranes and their mitigation strategies: a review, Sustainable Energy Fuels. 1 (2017) 409–438. https://doi.org/10.1039/C7SE00038C.

[5] A. Collier, H. Wang, X. Zi Yuan, J. Zhang, D.P. Wilkinson, Degradation of polymer electrolyte membranes, International Journal of Hydrogen Energy. 31 (2006) 1838–1854. https://doi.org/10.1016/j.ijhydene.2006.05.006.

[6] F.A. de Bruijn, V. a. T. Dam, G.J.M. Janssen, Review: Durability and Degradation Issues of PEM Fuel Cell Components, Fuel Cells. 8 (2008) 3–22. https://doi.org/10.1002/fuce.200700053.

[7] M.P. Rodgers, L.J. Bonville, H.R. Kunz, D.K. Slattery, J.M. Fenton, Fuel Cell Perfluorinated Sulfonic Acid Membrane Degradation Correlating Accelerated Stress Testing and Lifetime, Chem. Rev. 112 (2012) 6075–6103. https://doi.org/10.1021/cr200424d.

[8] A.B. LaConti, M. Hamdan, R.C. McDonald, Mechanisms of membrane degradation, in: Handbook of Fuel Cells, 2nd ed., John Wiley & Sons, Ltd, Hoboken, NJ (USA), 2010. https://doi.org/10.1002/9780470974001.f303055.

[9] M. Danilczuk, F.D. Coms, S. Schlick, Visualizing Chemical Reactions and Crossover Processes in a Fuel Cell Inserted in the ESR Resonator: Detection by Spin Trapping of Oxygen Radicals, Nafion-Derived Fragments, and Hydrogen and Deuterium Atoms, J. Phys. Chem. B. 113 (2009) 8031–8042. https://doi.org/10.1021/jp901597f.

[10] S.-Y. Lee, E. Cho, J.-H. Lee, H.-J. Kim, T.-H. Lim, I.-H. Oh, J. Won, Effects of Purging on the Degradation of PEMFCs Operating with Repetitive On/Off Cycles, J. Electrochem. Soc. 154 (2007) B194–B200. https://doi.org/10.1149/1.2403083.

[11] J. Healy, C. Hayden, T. Xie, K. Olson, R. Waldo, A. Brundage, H. Gasteiger, J. Abbott, Aspects of the Chemical Degradation of PFSA Ionomers used in PEM Fuel Cells, Fuel Cells. 5 (2005) 302–308. https://doi.org/10.1002/fuce.200400050.

[12] G.D. Moor, C. Bas, N. Charvin, E. Moukheiber, F. Niepceron, N. Breilly, J. André, E. Rossinot, E. Claude, N.D. Albérola, L. Flandin, Understanding Membrane Failure in PEMFC: Comparison of Diagnostic Tools at Different Observation Scales, Fuel Cells. 12 (2012) 356–364. https://doi.org/10.1002/fuce.201100161.

[13] C.S. Gittleman, F.D. Coms, Y.-H. Lai, Chapter 2 - Membrane Durability: Physical and Chemical Degradation, in: M.M. Mench, E.C. Kumbur, T.N. Veziroglu (Eds.), Polymer

Electrolyte Fuel Cell Degradation, Academic Press, Boston, 2012: pp. 15–88. https://doi.org/10.1016/B978-0-12-386936-4.10002-8.
[14] A. Kusoglu, A.M. Karlsson, M.H. Santare, S. Cleghorn, W.B. Johnson, Mechanical response of fuel cell membranes subjected to a hygro-thermal cycle, Journal of Power Sources. 161 (2006) 987–996. https://doi.org/10.1016/j.jpowsour.2006.05.020.
[15] A. Kusoglu, A.M. Karlsson, M.H. Santare, S. Cleghorn, W.B. Johnson, Mechanical behavior of fuel cell membranes under humidity cycles and effect of swelling anisotropy on the fatigue stresses, Journal of Power Sources. 170 (2007) 345–358. https://doi.org/10.1016/j.jpowsour.2007.03.063.
[16] A. Kusoglu, M.H. Santare, A.M. Karlsson, Aspects of Fatigue Failure Mechanisms in Polymer Fuel Cell Membranes, J. Polym. Sci. Pt. B-Polym. Phys. 49 (2011) 1506–1517. https://doi.org/10.1002/polb.22336.
[17] N.S. Khattra, A.M. Karlsson, M.H. Santare, P. Walsh, F.C. Busby, Effect of time-dependent material properties on the mechanical behavior of PFSA membranes subjected to humidity cycling, Journal of Power Sources. 214 (2012) 365–376. https://doi.org/10.1016/j.jpowsour.2012.04.065.
[18] A. Kusoglu, A.Z. Weber, A Mechanistic Model for Pinhole Growth in Fuel-Cell Membranes during Cyclic Loads, J. Electrochem. Soc. 161 (2014) E3311–E3322. https://doi.org/10.1149/2.036408jes.
[19] S. Shi, X. Sun, Q. Lin, J. Chen, Y. Fu, X. Hong, C. Li, X. Guo, G. Chen, X. Chen, Fatigue crack propagation behavior of fuel cell membranes after chemical degradation, International Journal of Hydrogen Energy. (2020) S0360319920326884. https://doi.org/10.1016/j.ijhydene.2020.07.113.
[20] W. Yoon, X. Huang, Acceleration of Chemical Degradation of Perfluorosulfonic Acid Ionomer Membrane by Mechanical Stress: Experimental Evidence, ECS Trans. 33 (2010) 907–911. https://doi.org/10.1149/1.3484584.
[21] A. Kusoglu, M. Calabrese, A.Z. Weber, Effect of Mechanical Compression on Chemical Degradation of Nafion Membranes, ECS Electrochem. Lett. 3 (2014) F33–F36. https://doi.org/10.1149/2.008405eel.
[22] V.M. Ehlinger, A. Kusoglu, A.Z. Weber, Modeling Coupled Durability and Performance in Polymer-Electrolyte Fuel Cells: Membrane Effects, J. Electrochem. Soc. 166 (2019) F3255–F3267. https://doi.org/10.1149/2.0281907jes.
[23] C. Lim, L. Ghassemzadeh, F. Van Hove, M. Lauritzen, J. Kolodziej, G.G. Wang, S. Holdcroft, E. Kjeang, Membrane degradation during combined chemical and mechanical accelerated stress testing of polymer electrolyte fuel cells, Journal of Power Sources. 257 (2014) 102–110. https://doi.org/10.1016/j.jpowsour.2014.01.106.
[24] A.S. Alavijeh, M.-A. Goulet, R.M.H. Khorasany, J. Ghataurah, C. Lim, M. Lauritzen, E. Kjeang, G.G. Wang, R.K.N.D. Rajapakse, Decay in Mechanical Properties of Catalyst Coated Membranes Subjected to Combined Chemical and Mechanical Membrane Degradation, Fuel Cells. 15 (2015) 204–213. https://doi.org/10.1002/fuce.201400040.
[25] S. velan Venkatesan, C. Lim, S. Holdcroft, E. Kjeang, Progression in the Morphology of Fuel Cell Membranes upon Conjoint Chemical and Mechanical Degradation, J. Electrochem. Soc. 163 (2016) F637–F643. https://doi.org/10.1149/2.0671607jes.
[26] R. Mukundan, A.M. Baker, A. Kusoglu, P. Beattie, S. Knights, A.Z. Weber, R.L. Borup, Membrane Accelerated Stress Test Development for Polymer Electrolyte Fuel Cell Durability Validated Using Field and Drive Cycle Testing, J. Electrochem. Soc. 165 (2018) F3085–F3093. https://doi.org/10.1149/2.0101806jes.
[27] Y. Singh, F.P. Orfino, M. Dutta, E. Kjeang, 3D visualization of membrane failures in fuel cells, Journal of Power Sources. 345 (2017) 1–11. https://doi.org/10.1016/j.jpowsour.2017.01.129.

[28] D. Ramani, Y. Singh, F.P. Orfino, M. Dutta, E. Kjeang, Characterization of Membrane Degradation Growth in Fuel Cells Using X-ray Computed Tomography, J. Electrochem. Soc. 165 (2018) F3200–F3208. https://doi.org/10.1149/2.0251806jes.
[29] K.-D. Kreuer, S.J. Paddison, E. Spohr, M. Schuster, Transport in Proton Conductors for Fuel-Cell Applications: Simulations, Elementary Reactions, and Phenomenology, Chem. Rev. 104 (2004) 4637–4678. https://doi.org/10.1021/cr020715f.
[30] T.A. Zawodzinski, T.E. Springer, F. Uribe, S. Gottesfeld, Characterization of polymer electrolytes for fuel cell applications, Solid State Ionics. 60 (1993) 199–211. https://doi.org/10.1016/0167-2738(93)90295-E.
[31] G. Gebel, P. Aldebert, M. Pineri, Swelling Study of Perfluorosulphonated Ionomer Membranes, Polymer. 34 (1993) 333–339. https://doi.org/10.1016/0032-3861(93)90086-P.
[32] M. Eikerling, A.A. Kornyshev, E. Spohr, Proton-Conducting Polymer Electrolyte Membranes: Water and Structure in Charge, in: G.G. Scherer (Ed.), Fuel Cells I, Springer, Berlin, Heidelberg, 2008: pp. 15–54. https://doi.org/10.1007/12_2008_132.
[33] A. Kusoglu, A.Z. Weber, New Insights into Perfluorinated Sulfonic-Acid Ionomers, Chem. Rev. 117 (2017) 987–1104. https://doi.org/10.1021/acs.chemrev.6b00159.
[34] C. D'Urso, C. Oldani, V. Baglio, L. Merlo, A.S. Aricò, Towards fuel cell membranes with improved lifetime: Aquivion® Perfluorosulfonic Acid membranes containing immobilized radical scavengers, Journal of Power Sources. 272 (2014) 753–758. https://doi.org/10.1016/j.jpowsour.2014.09.045.
[35] M. Zatoń, B. Prélot, N. Donzel, J. Rozière, D.J. Jones, Migration of Ce and Mn Ions in PEMFC and Its Impact on PFSA Membrane Degradation, J. Electrochem. Soc. 165 (2018) F3281–F3289. https://doi.org/10.1149/2.0311806jes.
[36] M.P. Rodgers, L.J. Bonville, R. Mukundan, R.L. Borup, R. Ahluwalia, P. Beattie, R.P. Brooker, N. Mohajeri, H.R. Kunz, D.K. Slattery, J.M. Fenton, Perfluorinated Sulfonic Acid Membrane and Membrane Electrode Assembly Degradation Correlating Accelerated Stress Testing and Lifetime Testing, ECS Trans. 58 (2013) 129–148. https://doi.org/10.1149/05801.0129ecst.
[37] G. De Moor, C. Bas, N. Charvin, J. Dillet, G. Maranzana, O. Lottin, N. Caque, E. Rossinot, L. Flandin, Perfluorosulfonic acid membrane degradation in the hydrogen inlet region: A macroscopic approach, Int. J. Hydrog. Energy. 41 (2016) 483–496. https://doi.org/10.1016/j.ijhydene.2015.10.066.
[38] M. Robert, A. El Kaddouri, J.-C. Perrin, S. Leclerc, O. Lottin, Towards a NMR-Based Method for Characterizing the Degradation of Nafion XL Membranes for PEMFC, J. Electrochem. Soc. 165 (2018) F3209–F3216. https://doi.org/10.1149/2.0231806jes.
[39] M. Robert, A. El Kaddouri, J.-C. Perrin, K. Mozet, M. Daoudi, J. Dillet, J.-Y. Morel, S. André, O. Lottin, Effects of conjoint mechanical and chemical stress on perfluorosulfonic-acid membranes for fuel cells, Journal of Power Sources. 476 (2020) 228662. https://doi.org/10.1016/j.jpowsour.2020.228662.
[40] F. Xu, C. Innocent, B. Bonnet, D.J. Jones, J. Roziere, Chemical modification of perfluorosulfonated membranes with pyrrole for fuel cell application: Preparation, characterisation and methanol transport, Fuel Cells. 5 (2005) 398–405. https://doi.org/10.1002/fuce.200400077.
[41] S.H. Frensch, G. Serre, F. Fouda-Onana, H.C. Jensen, M.L. Christensen, S.S. Araya, S.K. Kær, Impact of iron and hydrogen peroxide on membrane degradation for polymer electrolyte membrane water electrolysis: Computational and experimental investigation on fluoride emission, Journal of Power Sources. 420 (2019) 54–62. https://doi.org/10.1016/j.jpowsour.2019.02.076.

[42] M. Robert, A. El Kaddouri, J.-C. Perrin, J. Raya, O. Lottin, Time-resolved monitoring of composite Nafion™ XL membrane degradation induced by Fenton's reaction, Journal of Membrane Science. 621 (2021) 118977. https://doi.org/10.1016/j.memsci.2020.118977.
[43] E.O. Stejskal, J.E. Tanner, Spin Diffusion Measurements: Spin Echoes in the Presence of a Time- Dependent Field Gradient, The Journal of Chemical Physics. 42 (1965) 288–292. https://doi.org/10.1063/1.1695690.
[44] Y. Tang, A. Kusoglu, A.M. Karlsson, M.H. Santare, S. Cleghorn, W.B. Johnson, Mechanical properties of a reinforced composite polymer electrolyte membrane and its simulated performance in PEM fuel cells, Journal of Power Sources. 175 (2008) 817–825. https://doi.org/10.1016/j.jpowsour.2007.09.093.
[45] N.S. Khattra, Z. Lu, A.M. Karlsson, M.H. Santare, F.C. Busby, T. Schmiedel, Time-dependent mechanical response of a composite PFSA membrane, Journal of Power Sources. 228 (2013) 256–269. https://doi.org/10.1016/j.jpowsour.2012.11.116.
[46] E. Moukheiber, C. Bas, L. Flandin, Understanding the formation of pinholes in PFSA membranes with the essential work of fracture (EWF), Int. J. Hydrog. Energy. 39 (2014) 2717–2723. https://doi.org/10.1016/j.ijhydene.2013.03.031.
[47] Q. Lin, Z. Liu, L. Wang, X. Chen, S. Shi, Fracture property of Nafion XL composite membrane determined by R-curve method, Journal of Power Sources. 398 (2018) 34–41. https://doi.org/10.1016/j.jpowsour.2018.07.052.
[48] Z. Zhang, S. Shi, Q. Lin, L. Wang, Z. Liu, P. Li, X. Chen, Exploring the role of reinforcement in controlling fatigue crack propagation behavior of perfluorosulfonic-acid membranes, International Journal of Hydrogen Energy. 43 (2018) 6379–6389. https://doi.org/10.1016/j.ijhydene.2018.02.034.
[49] K. Hongsirikarn, X. Mo, J.G. Goodwin, S. Creager, Effect of H2O2 on Nafion® properties and conductivity at fuel cell conditions, Journal of Power Sources. 196 (2011) 3060–3072. https://doi.org/10.1016/j.jpowsour.2010.11.133.
[50] S. Kundu, L.C. Simon, M.W. Fowler, Comparison of two accelerated Nafion™ degradation experiments, Polymer Degradation and Stability. 93 (2008) 214–224. https://doi.org/10.1016/j.polymdegradstab.2007.10.001.
[51] S. Mu, C. Xu, Q. Yuan, Y. Gao, F. Xu, P. Zhao, Degradation behaviors of perfluorosulfonic acid polymer electrolyte membranes for polymer electrolyte membrane fuel cells under varied acceleration conditions, J. Appl. Polym. Sci. 129 (2013) 1586–1592. https://doi.org/10.1002/app.38785.
[52] H. Tang, S. Peikang, S.P. Jiang, F. Wang, M. Pan, A degradation study of Nafion proton exchange membrane of PEM fuel cells, Journal of Power Sources. 170 (2007) 85–92. https://doi.org/10.1016/j.jpowsour.2007.03.061.
[53] A.C. Fernandes, E.A. Ticianelli, A performance and degradation study of Nafion 212 membrane for proton exchange membrane fuel cells, Journal of Power Sources. 193 (2009) 547–554. https://doi.org/10.1016/j.jpowsour.2009.04.038.
[54] S. Schlick, G. Gebel, M. Pineri, F. Volino, Fluorine-19 NMR spectroscopy of acid Nafion membranes and solutions, Macromolecules. 24 (1991) 3517–3521. https://doi.org/10.1021/ma00012a008.
[55] G. Meresi, Y. Wang, A. Bandis, P.T. Inglefield, A.A. Jones, W.-Y. Wen, Morphology of dry and swollen perfluorosulfonate ionomer by fluorine-19 MAS, NMR and xenon-129 NMR, Polymer. 42 (2001) 6153–6160. https://doi.org/10.1016/S0032-3861(01)00053-2.
[56] Q. Chen, K. Schmidt-Rohr, F-19 and C-13 NMR signal assignment and analysis in a perfluorinated ionomer (Nafion) by two-dimensional solid-state NMR, Macromolecules. 37 (2004) 5995–6003. https://doi.org/10.1021/ma049759b.

[57] E. Moukheiber, G. De Moor, L. Flandin, C. Bas, Investigation of ionomer structure through its dependence on ion exchange capacity (IEC), J. Membr. Sci. 389 (2012) 294–304. https://doi.org/10.1016/j.memsci.2011.10.041.
[58] DuPont Product Information: Nafion NR-211 and NR-212 PFSA membrane, 2008., (n.d.). http://www.fuelcellsetc.com/store/DS/N211-N212-properties.pdf.
[59] S. Shi, A.Z. Weber, A. Kusoglu, Structure/property relationship of Nafion XL composite membranes, Journal of Membrane Science. 516 (2016) 123–134. https://doi.org/10.1016/j.memsci.2016.06.004.
[60] K.D. Baik, B.K. Hong, M.S. Kim, Effects of operating parameters on hydrogen crossover rate through Nafion® membranes in polymer electrolyte membrane fuel cells, Renewable Energy. 57 (2013) 234–239. https://doi.org/10.1016/j.renene.2013.01.046.
[61] P. Chippar, K. Oh, W.-G. Kim, H. Ju, Numerical analysis of effects of gas crossover through membrane pinholes in high-temperature proton exchange membrane fuel cells, International Journal of Hydrogen Energy. 39 (2014) 2863–2871. https://doi.org/10.1016/j.ijhydene.2013.05.117.
[62] T. Matsuura, J. Chen, J.B. Siegel, A.G. Stefanopoulou, Degradation phenomena in PEM fuel cell with dead-ended anode, International Journal of Hydrogen Energy. 38 (2013) 11346–11356. https://doi.org/10.1016/j.ijhydene.2013.06.096.
[63] S. Hommura, K. Kawahara, T. Shimohira, Y. Teraoka, Development of a Method for Clarifying the Perfluorosulfonated Membrane Degradation Mechanism in a Fuel Cell Environment, J. Electrochem. Soc. 155 (2008) A29–A33. https://doi.org/10.1149/1.2800171.
[64] G. Mousa, J. DeVaal, F. Golnaraghi, Diagnosis of hydrogen crossover and emission in proton exchange membrane fuel cells, International Journal of Hydrogen Energy. 39 (2014) 20116–20126. https://doi.org/10.1016/j.ijhydene.2014.09.116.
[65] J. Durst, A. Lamibrac, F. Charlot, J. Dillet, L.F. Castanheira, G. Maranzana, L. Dubau, F. Maillard, M. Chatenet, O. Lottin, Degradation heterogeneities induced by repetitive start/stop events in proton exchange membrane fuel cell: Inlet vs. outlet and channel vs. land, Appl. Catal. B-Environ. 138 (2013) 416–426. https://doi.org/10.1016/j.apcatb.2013.03.021.